



Cite this: *Chem. Commun.*, 2018, 54, 13252

Received 28th September 2018,
Accepted 1st November 2018

DOI: 10.1039/c8cc07761d

rsc.li/chemcomm

A highly selective and sensitive fluorescent probe for simultaneously distinguishing and sequentially detecting H₂S and various thiol species in solution and in live cells†

Dan Qiao,^a Tangliang Shen,^a Mengyuan Zhu,^b Xiao Liang,^a Lu Zhang,^a Zheng Yin,^a Binghe Wang ^{*b} and Luqing Shang ^{*a}

A novel dual-channel fluorescent probe (NCR) based on differences in reactivity among H₂S, Cys/Hcy, and GSH was rationally designed for simultaneously distinguishing and sequentially sensing H₂S, Cys/Hcy, and GSH using two emission channels, which also demonstrated that NCR can be used for targeting mitochondria in mammalian cells.

Thiol-containing amino acids and biomolecules, including cysteine (Cys), homocysteine (Hcy) and glutathione (GSH), play vital roles in physiological and pathological processes.¹ Hydrogen sulfide (H₂S) is recognized as an important gasotransmitter and plays an important role in human physiology.² H₂S levels are tightly associated with the levels of Cys, Hcy, and GSH in living systems, as endogenous H₂S can be produced from Cys and Hcy by cystathionine β-synthase and cystathionine γ-lyase.³ Abnormal cellular H₂S levels are implicated in many diseases such as Alzheimer's disease,⁴ Down's syndrome,⁵ and liver cirrhosis⁶ among others. Cys is an essential amino acid for the synthesis of proteins with its normal intracellular concentration in the range of 30–200 μM.⁷ Abnormal levels of Cys are related to retarded growth, hair depigmentation, edema, lethargy, liver damage, and cardiovascular diseases.⁸ The role of Hcy in diseases is a controversial topic and the normal concentration of Hcy in serum is approximately 5–15 μM.⁹ Elevated levels of Hcy in plasma are a risk factor for Alzheimer's and cardiovascular diseases.¹⁰ GSH is the most abundant intracellular thiol with intracellular concentrations in the range of 1–10 mM,¹¹ and is well-known to be associated with a number of disorders including cancer, Alzheimer's disease and other ailments.¹² Furthermore, the disulfide form of GSH

(GSSG) is involved in protein modification and consequently signal transduction.¹³ Therefore, assessment of the levels of these biothiols in biological systems in an integrated fashion is important for understanding their respective biological roles as well as their interplays in human physiology and pathology. Owing to the similar chemical structures and properties of these biothiols, it is challenging to simultaneously detect and discriminate Cys/Hcy, GSH, and H₂S from each other using a single agent.

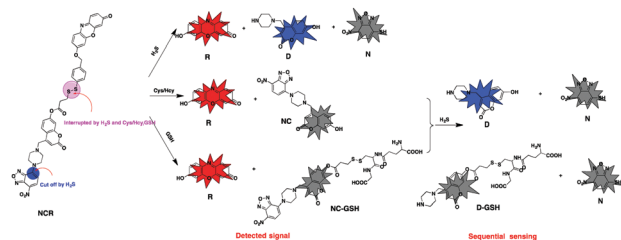
High-performance liquid chromatography (HPLC), capillary electrophoresis, spectrophotometry, mass spectrometry (MS), capillary electrophoresis and HPLC-MS/MS have been used previously for the detection and determination of specific biothiols.¹⁴ However, such methods do not address the issue of intracellular concentration, and yet the ability to detect and discriminate various biothiol species intracellularly is critical to the understanding of detailed sulfur biology. Fluorescence imaging techniques have attracted much attention owing to their simplicity, high sensitivity, non-invasiveness, and real-time detection in living systems.¹⁵ A number of fluorescent probes have been developed in recent years to detect and distinguish Cys/Hcy, GSH and H₂S.¹⁶ Lin and co-workers designed a fluorescent probe that could simultaneously distinguish Cys/Hcy, GSH, and H₂S, and sense them using a multi-channel fluorescence mode.¹⁷ A chlorinated coumarin-hemicyanine probe was developed with three potential reaction sites for simultaneous detection of Cys, Hcy and GSH using different emission channels.¹⁸ To the best of our knowledge, a single molecule fluorescent probe that can simultaneously detect and distinguish H₂S and various biothiols in solution and in live cells is quite rare (Table S1, ESI†).

In this work, we describe a novel fluorescent probe (NCR) with two potential reaction sites for simultaneously distinguishing and sequentially sensing H₂S, Cys/Hcy, and GSH from two emission channels. The design of the probe is based on different reaction mechanisms between the probe and H₂S, Cys/Hcy or GSH (Scheme 1). The probe NCR consists of two

^a College of Pharmacy, State Key Laboratory of Medicinal Chemical Biology and Tianjin Key Laboratory of Molecular Drug Research, Nankai University, Tianjin 300071, P. R. China. E-mail: shanglq@nankai.edu.cn

^b Department of Chemistry, Georgia State University, Atlanta, Georgia 30303, USA. E-mail: wang@gsu.edu

† Electronic supplementary information (ESI) available. See DOI: 10.1039/c8cc07761d



Scheme 1 The design strategy of the probe **NCR** and the proposed fluorescence signal changes in response to H_2S and biothiols or sequentially distinguishing Cys/Hcy and GSH due to the FRET effect between NBD and coumarin.

fluorophores, coumarin and resorufin, and a functional nitrobenzoxadiazole (NBD) moiety for the sequential sensing of biothiols (Cys/Hcy and GSH). The disulfide bond is used to connect coumarin and resorufin as the recognition unit for the selective response to H_2S and biothiols. In previous works, fluorescent probes with disulfide bonds as linkers or recognition groups were mainly used in prodrug preparation,¹⁹ thio-redoxin reductase-based activation,²⁰ H_2O_2 responsive prodrug,²¹ and preparation of precursors of H_2S ²² or biothiols.²³ A disulfide bond as a cleavable linker is particularly attractive, because of its stability in most blood pools and yet strong propensity to react with H_2S or other biothiols, leading to disulfide cleavage.^{19e} When a disulfide bond is linked to fluorophores, changes in emission intensity or shifts in the emission maxima often occur upon its cleavage, as a result of perturbation to the internal charge transfer (ICT) process. Moreover, probe **NCR** has additional desirable features, such as high water-solubility, large separation of the emission wavelengths (121 nm), and the ability to image biothiols in the mitochondria.

Herein, the **NCR** probe is inherently non-fluorescent due to the internal charge transfer (ICT) process and the quenching of the fluorescence of the coumarin moiety due to the FRET effect of NBD.²⁴ In the NBD chromophore, the carbon–nitrogen bond at the 4-position is easily cleaved by H_2S , due to the 7-position nitro group.²⁵ The product 4-thiol-7-nitro-benzofurazan (NBD-SH) is non-fluorescent, but the coumarin can emit fluorescence as a result of FRET removal. Thus, many NBD amine derivatives have been reported for the selective detection of H_2S .²¹ Additionally, the disulfide bond between coumarin and resorufin can be interrupted by nucleophilic reagents (e.g. biothiols). In the presence of H_2S , the NBD moiety is quickly released in the form of NBD-SH (**N**) and the disulfide bond is cleaved by the nucleophilic attack of H_2S . The cleavage of the disulfide linkage triggers the release of the free resorufin (**R**) through a quinone methide intermediate, and the subsequent lactonization of the persulfide species releases piperazine–coumarin (**D**). As a result, both blue and red emissions occur. However, reaction of the probe **NCR** with Cys/Hcy or GSH is expected to only produce **R**, and dark **NC** or **NC-GSH**. It is expected that the NBD would not be cleaved. As a result, only red emission from **R** is expected. If the reaction only stops at this stage, it appears to be difficult to discriminate between Cys/Hcy and GSH, because products **NC** and **NC-GSH** are expected to exhibit similar photophysical properties. However, when the dark products **NC**

and **NC-GSH** are subsequently treated with H_2S , NBD would be cleaved to yield **D** and dark **D-GSH** from **NC-GSH**. On the other hand, the addition of H_2S to **NC** is expected to result in blue emission as shown in Schemes S2 and S3 (ESI[†]). Taken together, the probe **NCR** is capable of not only simultaneously distinguishing H_2S and biothiols, but also sequentially sensing Cys/Hcy and GSH through two well-defined emission bands. As shown in Scheme S1 (ESI[†]), **NCR** was synthesized through several steps in desirable yield. All new compounds were fully characterized by ^1H NMR, ^{13}C NMR and HRMS (Fig. S20–S34, ESI[†]).

With the target probe **NCR**, we first investigated its sensing behavior towards H_2S , Cys/Hcy, and GSH in PBS at room temperature. As expected, free **NCR** (10 μM) exhibited no fluorescence in the visible region. Upon addition of an increasing amount of H_2S (from 0 to 100 equiv.), the mixture exhibited two new blue and red emission bands centered at 467 nm and 588 nm, respectively (Fig. 1A). The newly generated emission is ascribed to the release of free **R** and **D** as designed. Responding to Cys/Hcy and GSH (from 0 to 100 equiv.), only a gradual increase of the red emission was observed without the blue emission (Fig. 1B–D), indicating that the reaction of the probe with biothiols generated red fluorescent **R** and dark **NC** or **NC-GSH** because of the FRET effect between coumarin and NBD. With the concentration-dependent fluorescence intensity reaching the maximum values, H_2S induced a 125- and 83-fold enhancement of the fluorescence intensity at 467/588 nm, respectively. Cys, Hcy and GSH induced a 65, 65 and 70-fold enhancement of intensity at 588 nm, respectively (Fig. S1, ESI[†]). In addition, we also measured the fluorescence spectra of **NCR** upon successive

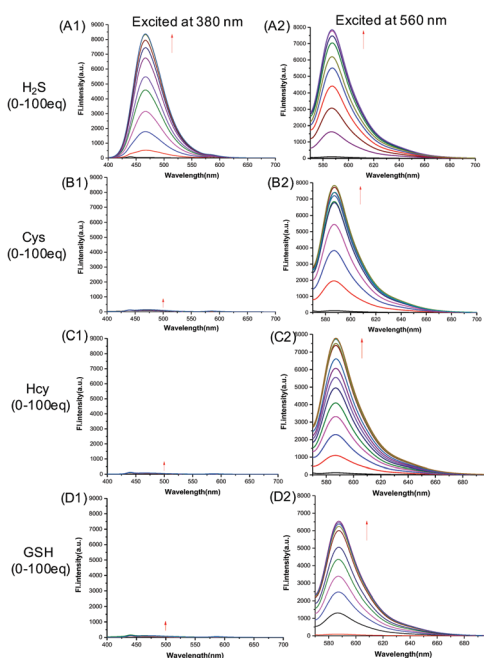


Fig. 1 The titration fluorescence spectra of **NCR** (10 μM) upon addition of (A) H_2S (0–100 equiv.), (B) Cys (0–100 equiv.), (C) Hcy (0–100 equiv.), and (D) GSH (0–100 equiv.) in DMSO/PBS buffer (25 mM, pH 7.4, 1:99 v/v.). $\lambda_{\text{ex}} = 380$ nm and $\lambda_{\text{em}} = 467$ nm for the first column. $\lambda_{\text{ex}} = 560$ nm and $\lambda_{\text{em}} = 588$ nm for the second column.

addition of Cys/Hcy/GSH, and H₂S in aqueous solution (Fig. S2, ESI[†]). Therefore, we can sequentially distinguish Cys/Hcy and GSH in terms of the fluorescence spectra at 467 nm.

Furthermore, fluorescence titration experiments under the same conditions were conducted. H₂S and biothiols have good linear relationships over a certain concentration range with the maximum intensity values of newly generated red emission bands. The detection limits were calculated to be 0.31 μM (H₂S), 0.27 μM (Cys), 0.45 μM (Hcy) and 0.46 μM (GSH) (Fig. S3, S4, ESI[†]).

To shed light on the response process, the absorption spectra of **NCR** were also investigated in aqueous solution (Fig. S5, ESI[†]). The extinction coefficient is as high as 29 083 M⁻¹ cm⁻¹ (Fig. S6, ESI[†]). ¹H-NMR titration experiments to further characterise the reaction were conducted (Fig. S7 and S8, ESI[†]). Furthermore, the mass spectra of **NCR** in H₂S and biothiols were measured in order to confirm the proposed reaction processes (Fig. S9–15, ESI[†]).

Encouraged by these results, we further evaluated the selectivity of probe **NCR** over other biologically related species (Fig. S16A, ESI[†]). This suggests that probe **NCR** can selectively detect H₂S, Cys/Hcy and GSH, without interference from relevant amino acids, representative anions, cations and ROS through changes in two well-defined emission bands. The effects of pH on the response of the probe **NCR** to H₂S and the respective biothiols were also assessed (Fig. S16B, ESI[†]), and the probe shows good response and allows for discrimination among H₂S and biothiols under near neutral pH conditions.

According to the calculation in the optimized structures of fluorescent probe (Fig. S17, ESI[†]), the response emission of **NCR** to H₂S and biothiols is regulated by the FRET and ICT mechanisms together.

Prior to applying the probe for the biological imaging, we assessed the cytotoxicity of **NCR** with HeLa cells by the MTT method. The results illustrated that the probe has low cytotoxicity at concentrations up to 20 μM (cell viability >85%) (Fig. S18, ESI[†]), which suggests that the probe is safe for visualizing H₂S and biothiols in live cells. To confirm the capability of the probe in detecting H₂S and biothiols, HeLa cells were incubated with 5.0 μM probe **NCR**. As predicted, the **NCR** loaded HeLa cells showed a bright emission in the red channel (Fig. 2A), which indicated that **NCR** reacted with the cellular biothiols and produced a strongly fluorescent resorufin chromophore. In the control experiment, after being pretreated with *N*-ethylmaleimide (NEM, a thiol scavenger, 0.5 mM), the **NCR** loaded HeLa cells exhibited very dim fluorescence in the two channels (Fig. 2B), which was in agreement with the emission spectral performance of the free probe in an aqueous system. For the experimental groups, the cells continued to be incubated with the respective exogenous H₂S and biothiols after being pre-treated with NEM for 30 min. Upon continuous treatment with H₂S (500 μM), a significant enhancement of fluorescence in both the blue and red channels was observed in the cells loaded with **NCR** (Fig. 2C). However, for continuous treatment of the cells with Cys/Hcy and GSH (500 μM), only an enhancement of fluorescence in the red channel was represented in the cells loaded with **NCR** (Fig. 2D–F). Therefore, **NCR** can discriminate cellular H₂S, Cys/Hcy, and GSH with two

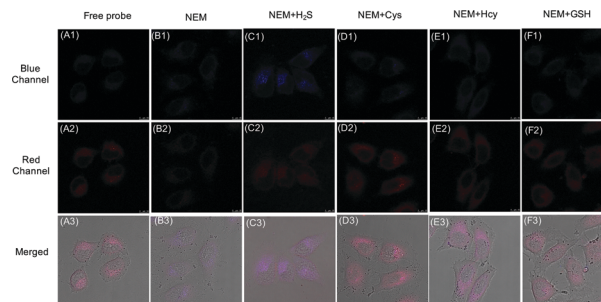


Fig. 2 Fluorescence images of probe **NCR** responding to the respective biothiols in living HeLa cells. Cells were incubated with (A) **NCR** (5 μM, 30 min); (B) NEM (0.5 mM, 30 min), subsequently incubated with probe **NCR** (5 μM, 30 min); (C) NEM (0.5 mM, 30 min), subsequently incubated with H₂S (500 μM, 30 min) and probe **NCR** (5 μM, 30 min); (D and E) NEM (0.5 mM, 30 min), subsequently incubated with Cys/Hcy (500 μM, 30 min) and probe **NCR** (5 μM, 30 min); and (F) NEM (0.5 mM, 30 min), subsequently incubated with GSH (500 μM, 30 min) and probe **NCR** (5 μM, 30 min) (blue channel of 440–490 nm and red channel of 575–620 nm). Scale bar: 10 μm.

different sets of fluorescence signals *via* dual-color fluorescence imaging.

Subsequently, to confirm the distribution of **NCR**, fluorescence co-localization experiments were carried out in HeLa cells using MitoTracker Green. The fluorescence image of **NCR** in the red channel almost completely overlapped with the commercial mitochondrial targeting dye in the green channel, with a high Pearson's correlation coefficient of 0.845 (Fig. S19, ESI[†]). This strongly indicated that probe **NCR** was able to penetrate into mitochondria.

Finally, the capabilities of probe **NCR** to selectively sense exogenous Cys/Hcy and GSH were evaluated in live cells. The cells were first treated with NEM to deactivate the cellular biothiols and SH-containing proteins. After incubation with **NCR**, almost no fluorescence could be observed (Fig. 3(A1–A3)). On the other hand, after being treated with Cys, Hcy and GSH, respectively, cells were incubated with **NCR** and subsequently treated with NaHS. Bright emission was observed in both the blue and red channels for the sample pretreated with Cys and Hcy (Fig. 3B and C). On the other hand, there was only a red emission band induced, without obvious fluorescence in the blue emission band in the sample pre-treated with GSH (Fig. 3D). Such results are consistent with the design principle and the solution test results. Hence, these results re-affirmed the selectivity of probe **NCR** for biothiols inside cells and also demonstrated the potential of probe **NCR** to sense intracellular Cys/Hcy and GSH simultaneously from dual-color fluorescence imaging in live cells.

In summary, by linking coumarin and resorufin with a disulfide bond and a nitrobenzoxadiazole (NBD) chromophore, we have designed a novel, water-soluble and mitochondria-targeted fluorescent probe (**NCR**), which could simultaneously detect and distinguish H₂S, Cys/Hcy, and GSH using two different emission channels. The fluorescence of probe **NCR** showed 65- to 125-fold increases in intensity with the addition of H₂S (467 and 588 nm) and biothiols (588 nm), respectively.

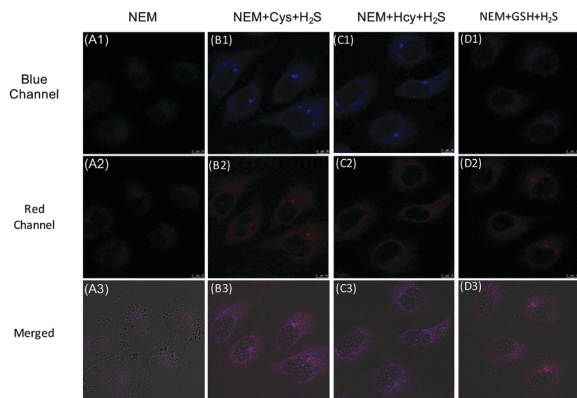


Fig. 3 Fluorescence images of probe **NCR** sequentially sensing Cys/Hcy, GSH and H_2S in living HeLa cells. Cells were incubated with (A) NEM (0.5 mM, 30 min), subsequently incubated with probe **NCR** (5 μM , 30 min); (B and C) NEM (0.5 mM, 30 min), subsequently incubated with Cys/Hcy (500 μM , 30 min) and probe **NCR** (5 μM , 30 min), continued to be treated with 500 μM NaHS for 30 min; and (D) NEM (0.5 mM, 30 min), subsequently incubated with GSH (500 μM , 30 min) and probe **NCR** (5 μM , 30 min), and continued to be treated with 500 μM NaHS for 30 min (blue channel of 440–490 nm and red channel of 575–620 nm). Scale bar: 10 μm .

The 121 nm separation in emission maxima between the blue and red channels allows for minimal or no signal overlap and high selectivity. Furthermore, fluorescence imaging studies in live cells demonstrated that probe **NCR** is able to simultaneously monitor endogenous and exogenous H_2S , Cys/Hcy, and GSH *via* dual-color imaging. This study may provide an effective tool for further exploration of the functions of various biothiol species in biological systems.

This work was supported by the National Key Research and Development Program of China (Grant No. 2018YFA0507204), the National Natural Science Foundation of China (Grant No. 21672115) and the State Key Laboratory of Medicinal Chemical Biology.

Conflicts of interest

There are no conflicts to declare.

Notes and references

- (a) S. Zhang, C. N. Ong and H. M. Shen, *Cancer Lett.*, 2004, **208**, 143–153; (b) S. Shahrokhian, *Anal. Chem.*, 2001, **73**, 5972–5978; (c) N. M. Giles, A. B. Watts, G. I. Giles, F. H. Fry, J. A. Littlechild and C. Jacob, *Chem. Biol.*, 2003, **10**, 677–693; (d) D. Giuliani, A. Ottani, D. Zaffe, M. Galantucci, F. Strinati, R. Lodi and S. Guarini, *Neurobiol. Learn. Mem.*, 2013, **104**, 82–91.
- (a) G. Yang, L. Wu, B. Jiang, W. Yang, J. Qi, K. Cao, Q. Meng, A. K. Mustafa, W. Mu, S. Zhang, S. H. Snyder and R. Wang, *Science*, 2008, **322**, 587–590; (b) C. Szabo, *Antioxid. Redox Signaling*, 2012, **17**, 68–80.
- S. Singh, D. Padovani, R. A. Leslie, T. Chiku and R. Banerjee, *J. Biol. Chem.*, 2009, **284**, 22457–22466.
- K. Eto, T. Asada, K. Arima, T. Makifuchi and H. Kimura, *Biochem. Biophys. Res. Commun.*, 2005, **333**, 1045.
- P. Kamoun, M. C. Belardinelli, A. Chabli, K. Lallouchi and B. Chadefaux-Vekemans, *Am. J. Med. Genet., Part A*, 2003, **116A**, 310–311.
- S. Fiorucci, E. Antonelli, A. Mencarelli, S. Orlandi, B. Renga, G. Rizzo, E. Distrutti, V. Shah and A. Morelli, *Hepatology*, 2005, **42**, 539–548.
- Y. Yue, F. Huo, P. Ning, Y. Zhang, J. Chao, X. Meng and C. Yin, *J. Am. Chem. Soc.*, 2017, **139**, 3181–3185.
- (a) W. Wang, O. Rusin, X. Xu, K. K. Kim, J. O. Escobedo, S. O. Fakayode, K. A. Fletcher, M. Lowry, C. M. Schowalter, C. M. Lawrence, F. R. Fronczek, I. M. Warner and R. M. Strongin, *J. Am. Chem. Soc.*, 2005, **127**, 15949–15958; (b) C. E. Paulsen and K. S. Carroll, *Chem. Rev.*, 2013, **113**, 4633–4679.
- H. Y. Lee, Y. P. Choi, S. Kim, T. Yoon, Z. Guo, S. Lee, K. M. Swamy, G. Kim, J. Y. Lee, I. Shin and J. Yoon, *Chem. Commun.*, 2014, **50**, 6967–6969.
- B. Debreceni and L. Debreceni, *Cardiovasc. Ther.*, 2014, **32**, 130–138.
- (a) S. S. M. Hassan and G. A. Rechnitz, *Anal. Chem.*, 1982, **54**, 1972–1976; (b) H. S. Jung, X. Chen, J. S. Kim and J. Yoon, *Chem. Soc. Rev.*, 2013, **42**, 6019–6031.
- (a) D. M. Townsend, K. D. Tew and H. Tapiero, *Biomed. Pharmacother.*, 2003, **57**, 145–155; (b) Y. Zhang, X. Shao, Y. Wang, F. Pan, R. Kang, F. Peng, Z. Huang, W. Zhang and W. Zhao, *Chem. Commun.*, 2015, **51**, 4245–4248.
- T. Ida, T. Sawa, H. Ihara, Y. Tsuchiya, Y. Watanabe, Y. Kumagai, M. Suematsu, H. Motohashi, S. Fujii, T. Matsunaga, M. Yamamoto, K. Ono, N. O. Devarie-Baez, M. Xian, J. M. Fukuto and T. Akaike, *Proc. Natl. Acad. Sci. U. S. A.*, 2014, **111**, 7606–7611.
- (a) J. Vacek, B. Klejdus, J. Petrlova, L. Lojkova and V. Kuban, *Analyst*, 2006, **131**, 1167–1174; (b) T. Inoue and J. R. Kirchhoff, *Anal. Chem.*, 2002, **74**, 1349–1354; (c) G. Liang, J. Ronald, Y. Chen, D. Ye, P. Pandit, M. L. Ma, B. Rutt and J. Rao, *Angew. Chem., Int. Ed. Engl.*, 2011, **50**, 6283–6286; (d) B. Seiwert and U. Karst, *Anal. Chem.*, 2007, **79**, 7131–7138.
- (a) J. Yin, Y. Hu and J. Yoon, *Chem. Soc. Rev.*, 2015, **44**, 4619–4644; (b) Q. Xu, C. H. Heo, G. Kim, H. W. Lee, H. M. Kim and J. Yoon, *Angew. Chem., Int. Ed. Engl.*, 2015, **54**, 4890–4894; (c) W. Chen, S. Xu, J. J. Day, D. Wang and M. Xian, *Angew. Chem., Int. Ed. Engl.*, 2017, **56**, 16611–16615; (d) X. Liang, X. Xu, D. Qiao, Z. Yin and L. Shang, *Chem. – Asian J.*, 2017, **12**, 3187–3194.
- J. Zhang, X. Ji, J. Zhou, Z. Chen, X. Dong and W. Zhao, *Sens. Actuators, B*, 2018, **257**, 1076–1082.
- L. He, X. Yang, K. Xu, X. Kong and W. Lin, *Chem. Sci.*, 2017, **8**, 6257–6265.
- (a) J. Liu, Y. Q. Sun, Y. Huo, H. Zhang, L. Wang, P. Zhang, D. Song, Y. Shi and W. Guo, *J. Am. Chem. Soc.*, 2014, **136**, 574–577; (b) G. X. Yin, T. T. Niu, Y. B. Gan, T. Yu, P. Yin, H. M. Chen, Y. Y. Zhang, H. T. Li and S. Z. Yao, *Angew. Chem., Int. Ed.*, 2018, **57**, 4991–4994.
- (a) S. Bhuniya, S. Maiti, E. J. Kim, H. Lee, J. L. Sessler, K. S. Hong and J. S. Kim, *Angew. Chem., Int. Ed. Engl.*, 2014, **53**, 4469–4474; (b) S. Maiti, N. Park, J. H. Han, H. M. Jeon, J. H. Lee, S. Bhuniya, C. Kang and J. S. Kim, *J. Am. Chem. Soc.*, 2013, **135**, 4567–4572; (c) Z. Yang, J. H. Lee, H. M. Jeon, J. H. Han, N. Park, Y. He, H. Lee, K. S. Hong, C. Kang and J. S. Kim, *J. Am. Chem. Soc.*, 2013, **135**, 11657–11662; (d) M. H. Lee, J. Y. Kim, J. H. Han, S. Bhuniya, J. L. Sessler, C. Kang and J. S. Kim, *J. Am. Chem. Soc.*, 2012, **134**, 12668–12674; (e) M. H. Lee, J. L. Sessler and J. S. Kim, *Acc. Chem. Res.*, 2015, **48**, 2935–2946.
- (a) M. H. Lee, H. M. Jeon, J. H. Han, N. Park, C. Kang, J. L. Sessler and J. S. Kim, *J. Am. Chem. Soc.*, 2014, **136**, 8430–8437; (b) L. Zhang, D. Duan, Y. Liu, C. Ge, X. Cui, J. Sun and J. Fang, *J. Am. Chem. Soc.*, 2014, **136**, 226–233.
- C. R. Powell, K. M. Dillon, Y. Wang, R. J. Carrazzone and J. B. Matson, *Angew. Chem., Int. Ed. Engl.*, 2018, **57**, 6324–6328.
- (a) B. Peng, W. Chen, C. Liu, E. W. Rosser, A. Pacheco, Y. Zhao, H. C. Aguilar and M. Xian, *Chemistry*, 2014, **20**, 1010–1016; (b) F. Yu, X. Han and L. Chen, *Chem. Commun.*, 2014, **50**, 12234–12249.
- C. S. Lim, G. Masanta, H. J. Kim, J. H. Han, H. M. Kim and B. R. Cho, *J. Am. Chem. Soc.*, 2011, **133**, 11132–11135.
- (a) Y. Tang and G.-F. Jiang, *New J. Chemistry*, 2017, **41**, 6769–6774; (b) Y. Huang, C. Zhang, Z. Xi and L. Yi, *Tetrahedron Lett.*, 2016, **57**, 1187–1191.
- F. Song, Z. Li, J. Li, S. Wu, X. Qiu, Z. Xi and L. Yi, *Org. Biomol. Chem.*, 2016, **14**, 11117–11124.